

Synthetic MC via Biological Transmitters: Therapeutic Modulation of the Gut-Brain Axis

Sebastian Lotter*, Elisabeth Mohr*, Andrina Rutsch†, Lukas Brand*, Francesca Ronchi†, Laura Díaz-Marugán†

*Friedrich-Alexander-Universität Erlangen-Nürnberg, Erlangen, Germany

†Charité – Universitätsmedizin Berlin, Humboldt-Universität zu Berlin, Berlin Institute of Health (BIH), Berlin, Germany

Abstract—Synthetic molecular communication (SMC) is a key enabler for future healthcare systems in which Internet of Bio-Nano-Things (IoBNT) devices facilitate the continuous monitoring of a patient’s biochemical signals. To close the loop between sensing and actuation in these systems, both the *detection* and the *generation* of in-body molecular communication (MC) signals is key. However, generating signals inside the human body, e.g., via synthetic nanodevices, still poses a major research challenge in SMC, due to technological obstacles as well as legal, safety, and ethical issues. In contrast to many existing studies, this paper considers an SMC system in which signals are generated *indirectly* via the modulation of a natural in-body MC system, namely the gut-brain axis (GBA). Therapeutic GBA modulation is already established as treatment for some neurological diseases, e.g., drug refractory epilepsy (DRE), and performed via the administration of nutritional supplements or specific diets with therapeutic effect. However, the molecular signaling pathways that mediate the effect of such treatments are mostly unknown. Consequently, existing treatments are standardized or designed heuristically and able to help only some patients while failing to help others. In this paper, we propose to leverage personal health data, e.g., data gathered by in-body IoBNT devices, to overcome this research gap and design more versatile and robust GBA modulation-based treatments as compared to the existing ones. To show the feasibility of our approach, we first define a catalog of theoretical requirements for therapeutic GBA modulation. Then, we propose a machine learning model to verify these requirements for practical scenarios when only limited data on the GBA modulation is available. By evaluating the proposed model on several published datasets, we confirm its excellent accuracy in identifying different modulators of the GBA. Finally, we utilize the proposed model to identify specific modulatory pathways that play an important role for therapeutic GBA modulation. The results presented in this paper may help to develop novel personalized GBA-based treatments, i.e., novel nutritional supplements and/or diets, to help patients that do not respond to existing standardized treatments.

I. INTRODUCTION

Synthetic molecular communication (SMC) is expected to facilitate early disease detection and treatment with the help of synthetic in-body nanodevices that operate in the *Internet of Bio-Nano-Things (IoBNT)* [1]. The IoBNT is a next-generation communication network that integrates conventional communication networks, such as the Internet, with nanoscale in-body communication devices, like nanorobots and synthetic cells. Conceptually, many of the disruptive healthcare applications enabled by SMC involve two main components: *sensing* and *actuation*. Here, sensing refers to the detection of natural molecular signals inside the human body. For example, biomarkers indicative of some disease can be sensed. The detected natural molecular communication (MC) signals can then be processed and interpreted either locally, i.e., in the

body, or remotely, i.e., after relaying them to computing devices outside the body and/or human specialists. If necessary, this can trigger personalized medical interventions.

In turn, actuation entails generating MC signals inside the human body to enable specific, targeted medical interventions. This signal generation can happen *directly* or *indirectly*. In direct signal generation, MC signals are generated by *engineered devices*, e.g., in-body nanorobots or synthetic cells, whereas *biological signal generators* are used to generate the MC signals in indirect signal generation. The direct generation of molecular signals for therapeutic applications has widely been researched in the MC literature in theory, especially in the context of targeted drug delivery and controlled release [2], [3]. However, the existing administrative and legal requirements render the admission of active (i.e., signal generating) in-body nanodevices for medical applications a challenging and potentially long-term process in practice. In contrast, this paper considers an SMC system in which the communication signals are generated indirectly, namely the gut-brain axis (GBA).

The GBA has been the subject of several studies in physiological and pathological conditions [4] and has already been identified as one promising research direction for SMC [5], [6]. Also, modulation of the GBA via dietary interventions and nutritional supplements is an established treatment for neurological disorders such as drug refractory epilepsy (DRE) [7]–[9]. However, it is currently not known how such modulation affects the generation of MC signals along the GBA, limiting the possibilities to adapt the treatment to the individual patient’s biochemical preconditions (e.g., their gut microbiome composition). Overcoming this lack of knowledge will facilitate the development of more robust and more effective treatments as compared to existing ones. In this paper, we showcase how personalized health data, such as that acquired by future IoBNT devices, can be used to understand the interaction between medical interventions and MC along the GBA (GBA-MC). Specifically, we utilize a novel information theoretical framework for GBA-MC to develop a computational tool that identifies main modulatory effects of dietary interventions on GBA-MC and confirm the accuracy of this tool with data from mice models. Specifically, this paper makes the following main contributions:

- An information theoretical framework for the indirect signal generation via modulation of a biological MC transmitter (Tx) is proposed for an MC system that is highly relevant for medical applications, namely the GBA.
- Based on the information theoretical framework, a novel

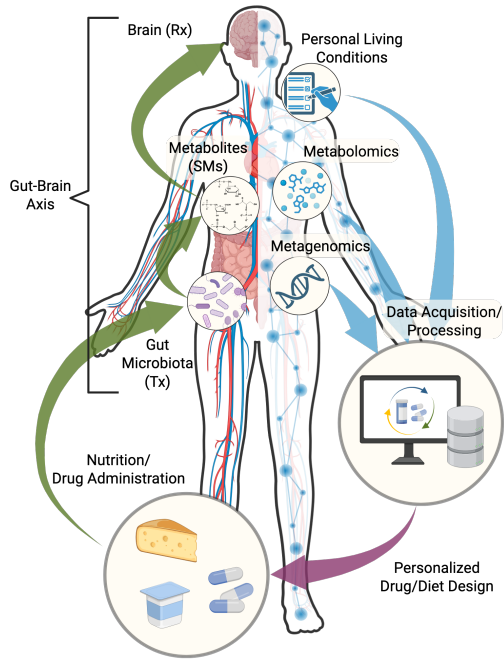


Figure 1. The integration of next-generation health data acquisition facilitated by the IoBNT (right, blue arrows) with therapeutical modulation of the GBA (left, green arrows) via personalized, data-informed drug/diet design (bottom, purple arrow). In GBA-MC, the gut microbiota acts as MC Tx producing metabolites as SMs that propagate through blood vessels and the blood-brain-barrier to the brain acting as the MC Rx.

computational model for the dietary modulation of GBA-MC based on a random forest (RF) classifier is presented.

- The proposed model is utilized to study the modulation of the GBA by specific dietary interventions under various conditions (e.g., health status) of the host.
- Main modulatory pathways are identified with respect to (w.r.t.) the gut bacteria and the associated metabolic signaling.

In summary, this paper presents a step towards closing the sensing-actuation loop in the IoBNT-assisted treatment of neurological disorders (as illustrated in Fig. 1). Due to the generality of the proposed framework, it can be adapted to the modulation of other biological MC systems.

The remainder of this paper is organized as follows. Section II introduces the relevant biological background on the GBA and its importance for the dietary treatment of neurodegenerative diseases. Section III introduces the novel information theoretical framework for GBA-MC. The proposed computational model is presented in Section IV and the utilized datasets are introduced in Section V. Finally, Section VI presents the main evaluation results and Section VII concludes the paper and outlines topics for future work.

II. GUT-BRAIN AXIS, DIETARY INTERVENTIONS, AND NEURODEGENERATIVE DISEASE

A. Background

The GBA is the multidirectional communication¹ between the intestine with commensal microbes (gut microbiota) and the central nervous system (CNS) with a profound influence on neurological disorders and neural development. The gut microbiota is a community of symbiotic microorganisms that reach a density of more than 10^{12} cells/g of content in the large intestine of mammals [10]. Under healthy conditions, the mucosal microbiota plays a vital role in food digestion, vitamin synthesis, physiological organ development, and protection against pathogens. Intestinal microbes have also been shown to be important in the CNS development. Alterations in the balance of host-microbial interactions in the gut, such as dysbiotic (altered in composition) microbiota, have been observed in various neurological disorders, such as major depressive and mood disorders, neurodegenerative, and neuropsychiatric disorders [11], [12].

Mounting evidence points towards gut microbiota as an essential mediator of dietary effects on the host organism [13]. Intestinal microbiota can affect the host responses through the dissemination of bacterial products or metabolites (substances produced during metabolism) and this is strongly dependent upon the substrates available through dietary intake [14]. Diet is, in fact, one of the major forces that shape the microbiota [15]–[17] in terms of composition and metabolism, contributing to host homeostasis and disease susceptibility. Currently, nutrition is a complementary and alternative approach in the management of neurological diseases, showing positive effects, especially in drug-resistant patients [8], [18], [19].

A dietary approach that has been shown to ameliorate several metabolic and neurological conditions, such as DRE, autism spectrum disorder, Alzheimer’s disease, and cancer is a *ketogenic diet (KD)*. KD, high in fat and low in carbohydrates, decreases glycemia and insulin levels, and increases the concentration of ketone bodies systemically. Recently, clinical and experimental studies suggested important effects of KD regimen on the host CNS via alterations of the microbiota. We will conceptualize these modulatory effects of KD on the GBA information theoretically in Section III. To exemplify first some major open research questions associated with KD-based treatment, we focus on the treatment of DRE in the following. DRE accounts for one third of the people with epilepsy and 80% of the total cost of treating the condition. People with DRE have been reported to have an enrichment of several microbes (e.g., *Clostridium XVIII*, *Dorea*, *Coprobaecillus*, *Ruminococcus*, *Akkermansia*, *Neisseria*, *Coprococcus* or *Actinobacteria*, *Verrucomicrobia*, *Nitrospirae*, *Blautia*, *Bifidobacterium*, *Subdoligranulum*, *Dialister*, and *Anaerostipes* [20], [21]), compared to drug-sensitive patients and healthy controls. In a study of 20 people affected by DRE, after six months of KD treatment, a quarter of the people had

¹We focus on the communication from gut to brain in this paper, hence, only this direction is illustrated in Fig. 1.

$\geq 90\%$ or complete seizure reduction, another quarter had seizure reduction of 50-89%, and half had $< 50\%$ reduction [22]. Indeed, treatment with KD can reduce seizure frequency by about 50% in about 50% of DRE cases that adhere to it. Animal and human studies suggest that gut microbiota is responsible for the benefits of this diet [9], [23]. Furthermore, Dahlin *et al.* identified associations between specific microbial species and serum metabolites associated with seizure reduction in people with DRE after KD intervention [24]. These data show the potential and the importance of deciphering how the diet and microbiota can modulate disease development in some individuals with beneficial or detrimental effects on the CNS health. However, causal relationships between the composition of the human gut microbiota and the therapeutic effect of KD remain elusive. Elucidating such relationships could help to predict and further improve the success rate of KD-based treatment and will pave the way for future therapies for various disorders. This is especially important since KD is a very restrictive diet with low acceptance or adherence to, and its long-term consumption could cause some adverse effects, such as nausea, vomiting, diarrhea, constipation, and weight loss.

B. Integration with the IoBNT

KD, as a specific therapeutic measure in the treatment of DRE, exemplifies (i) the enormous benefit for public health that would result from improving the efficiency of GBA-mediated therapies and (ii) that such improvements could possibly be achieved by better aligning the treatments with the individual gut microbiota composition of the host. Now, the IoBNT, in which the host's body functions are continuously monitored at unprecedented levels, enables access to metagenomic and metabolomic data that characterizes the state of the host's gut microbiome and its response to dietary interventions. Facilitated by this data (and by additional information on the host's living conditions, e.g., live habits, psychosocial factors), personalized treatments that are aligned with the host's gut microbiota come in reach. Fig. 1 illustrates this concept: data acquired by IoBNT devices is processed at central computing units and utilized to design personalized diets or nutritional supplements. When administered, such personalized treatments are not only expected to be more effective in the management of neurological diseases as compared to existing standardized treatments, their effect can also be sensed directly by the IoBNT devices which closes the loop by facilitating further adjustments of the treatment. Next, we present a feasibility study that demonstrates how the SMC framework can help to realize this vision.

III. SYSTEM MODEL AND PROBLEM FORMULATION

One major challenge in designing personalized dietary treatments or nutritional supplements for combating neurodegenerative diseases via the GBA is to identify the main signaling pathways by which externally controllable variables, such as the diet, impact communication along the GBA. In the following, we first introduce a formal framework for

gut microbiota-mediated signaling, before we formulate the inference problem that we will utilize later on to tackle this problem.

A. System Model

We model the concentrations of different bacterial species $i \in \mathcal{B}$ as random variables (RVs) $S_i \in \mathbb{R}_0^+$, where \mathcal{B} and \mathbb{R}_0^+ denote the set of bacterial species that are potentially present in the gut and the set of non-negative real numbers, respectively. In GBA-MC, the gut microbiome is regarded as Tx with associated state $\mathcal{S} = \{S_i\}$ that emits molecular signals composed of different metabolites (corresponding to SMs). Depending on \mathcal{S} , the *metabolic profiles*, i.e., the presence and absence of particular metabolites, of other parts of the human body vary. In GBA-MC, we are mostly interested in the metabolic profile of the serum, which we denote by $\mathcal{X}^s = \{X_k^s\}$, where $k \in \mathcal{M}$, \mathcal{M} denotes the set of metabolites, and RV $X_k^s \in \mathbb{R}_0^+$ denotes the concentration of metabolite k in the serum. Via the serum, in particular via \mathcal{X}^s , information is conveyed from the gut to the brain, cf. Section II. However, \mathcal{X}^s is subject to many other influences besides \mathcal{S} , such as the health status of the host. Hence, the statistical correlation between \mathcal{X}^s and \mathcal{S} may be obfuscated by interfering molecular signals, e.g., signals originating from cancerous tissue. Hence, as an additional readout for the metabolic activity of the gut microbiota, we consider in this paper also the metabolic profile of the colon, denoted as $\mathcal{X}^c = \{X_k^c\}$, where RV $X_k^c \in \mathbb{R}_0^+$ denotes the concentration of metabolite k in the colon. \mathcal{X}^c comprises the molecular signal released from the gut microbiota to the colon. Due to the spatial proximity between gut microbiota and colon metabolites, \mathcal{S} and \mathcal{X}^c are statistically strongly correlated.

Both, the gut microbiota itself (\mathcal{S}) and the metabolic signals modulated by it (\mathcal{X}^s and \mathcal{X}^c) are subject to multifactorial dependencies, among others, on the genetic identity, current constitution, and alimentation/diet of the host, cf. Section II. In this paper, we characterize some of these dependencies using previously published data from mice and statistical inference with the long-term goal to identify novel targets for therapeutic modulation of the GBA in the personalized treatment of neurodegenerative diseases.

To introduce the proposed approach rigorously in the following, we finally collect factors that are potentially statistically interdependent with \mathcal{S} , \mathcal{X}^s , or \mathcal{X}^c in the set of random variables $\mathcal{F} = \{F_j\}$, $j \in \mathbb{N}$. In the context of this paper, F_j are discrete-valued RVs indicating the value of any categorical variable. For example, F_j can denote the type of diet on which the host is fed or the type of disease (e.g., cancer type) it is infected with. However, the framework presented in this paper can easily be extended to continuous-valued F_j 's. The statistical interdependencies between \mathcal{F} on the one hand and \mathcal{S} , \mathcal{X}^c , and \mathcal{X}^s on the other hand are unknown in general and object of this study. Finally, we note that \mathcal{F} , \mathcal{S} , \mathcal{X}^c , and \mathcal{X}^s are distributed according to *population statistics*. Specifically, the randomness in \mathcal{F} , \mathcal{S} , \mathcal{X}^c , and \mathcal{X}^s represents the variability of the respective variables over a *population of hosts* (e.g., a group

of lab mice), *not* the statistics of their potential fluctuations over time in a single host. On a population level, time (e.g., the time elapsed since the start of a treatment/diet) is accounted for in the proposed model as one of the variables collected in \mathcal{F} ; this is the case, for example, in Dataset 1 (DS-1) as introduced in Section V.

B. Problem Formulation

From an information theoretical point of view, the information conveyed between two disjoint sets of RVs is measured in terms of their *mutual information (MI)*. Considering the two finite-sized sets $\mathbf{F} = \{F_{j_1}, \dots, F_{j_{|\mathbf{F}|}}\} \subseteq \mathcal{F}$ and $\mathbf{S} = \{S_{i_1}, \dots, S_{i_{|\mathbf{S}|}}\} \subseteq \mathcal{S}$, for example, where $|\mathbf{A}|$ denotes the cardinality of set \mathbf{A} , the MI, I , is defined as

$$I(\mathbf{F}; \mathbf{S}) = H(\mathbf{F}) - H(\mathbf{F} | \mathbf{S}) \quad (1)$$

$$= H(F_{j_1}, \dots, F_{j_{|\mathbf{F}|}}) - H(F_{j_1}, \dots, F_{j_{|\mathbf{F}|}} | S_{i_1}, \dots, S_{i_{|\mathbf{S}|}}),$$

where $H(\cdot)$ and $H(\cdot | \cdot)$ denote the entropy function and the conditional entropy function, respectively. Adopting this perspective, we define the concept of a *GBA modulator* as follows.

Definition 1 (GBA modulator): Any subset of influencing factors $\mathbf{F} \subseteq \mathcal{F}$ is a *modulator of \mathcal{S}* (*modulator of \mathcal{X}^s* , *modulator of \mathcal{X}^c*) if and only if there exists a non-empty, finite-sized subset $\mathbf{S} \subseteq \mathcal{S}$ ($\mathbf{X}^s \subseteq \mathcal{X}^s$, $\mathbf{X}^c \subseteq \mathcal{X}^c$) for which $I(\mathbf{F}; \mathbf{S}) > 0$ ($I(\mathbf{F}; \mathbf{X}^s) > 0$, $I(\mathbf{F}; \mathbf{X}^c) > 0$). If \mathbf{F} is a modulator of \mathcal{S} or \mathcal{X}^s , it is a *GBA modulator*.

Def. 1 unifies the two requirements that (i) \mathbf{F} is non-deterministic ($H(\mathbf{F}) > 0$), i.e., it varies over the considered population, and (ii) \mathbf{F} is correlated with the set of RVs it modulates. However, from a practical point of view, Def. 1 does not address two important aspects that are relevant for therapeutic modulation. For therapeutic modulation, first, the modulator \mathbf{F} as defined in Def. 1 needs to be controllable as part of a medical treatment and, second, it shall exhibit robust influence on the GBA as some other, non-controllable influencing factors vary. The following two definitions address these two points.

Definition 2 (Feasible GBA modulator): Any GBA modulator \mathbf{F} is a *feasible GBA modulator* if the values of all $F_{j_1}, \dots, F_{j_{|\mathbf{F}|}} \in \mathbf{F}$ can be set via human intervention.

Definition 3 (Robust GBA modulator): Any GBA modulator $\mathbf{F}_1 \subseteq \mathcal{F}$ is a *robust modulator of \mathcal{S}* (*robust modulator of \mathcal{X}^s* , *robust modulator of \mathcal{X}^c*) w.r.t. $\mathbf{F}_2 \subseteq \mathcal{F}$ if and only if $I(\mathbf{F}_1; \mathbf{S} | \mathbf{F}_2) = H(\mathbf{F}_1 | \mathbf{F}_2) - H(\mathbf{F}_1 | \mathbf{F}_2, \mathbf{S}) > 0$ ($I(\mathbf{F}_1; \mathbf{X}^s | \mathbf{F}_2) > 0$, $I(\mathbf{F}_1; \mathbf{X}^c | \mathbf{F}_2) > 0$), where \mathbf{S} , \mathbf{X}^s , and \mathbf{X}^c were defined in Def. 1. If \mathbf{F}_1 is a robust modulator of \mathcal{S} or \mathcal{X}^s w.r.t. \mathbf{F}_2 , it is called a *robust GBA modulator w.r.t. \mathbf{F}_2* .

A specific disease that interacts with the microbiome or the serum metabolites of the host, a cancer for example, can be a GBA modulator according to Def. 1, but not a feasible GBA modulator, cf. Def. 2, given that removing the disease is not available as a direct therapeutic option. Furthermore, for any \mathbf{F}_1 that is a robust GBA modulator w.r.t. \mathbf{F}_2 , Def. 3 implies $H(\mathbf{F}_1 | \mathbf{F}_2) > 0$, i.e., \mathbf{F}_2 cannot be a deterministic function of \mathbf{F}_1 , and (assuming without loss of generality that \mathbf{F}_1 modulates \mathcal{S}) $H(\mathbf{F}_1 | \mathbf{F}_2, \mathbf{S}) < H(\mathbf{F}_1 | \mathbf{F}_2)$, i.e., \mathbf{F}_1 , \mathbf{F}_2 , \mathbf{S} may *not* form

a Markov chain $\mathbf{F}_1 \rightarrow \mathbf{F}_2 \rightarrow \mathbf{S}$ or, in other words, \mathbf{F}_1 and \mathbf{S} may *not* be conditionally independent given \mathbf{F}_2 .

Now the problem in identifying feasible and robust GBA modulators according to Defs. 1-3 is that the conditional probabilities $\Pr\{\mathbf{F} | \mathbf{S}\}$ and $\Pr\{\mathbf{F} | \mathbf{X}^s\}$ are unknown and the MI is notoriously difficult to estimate from data whenever high-dimensional sets of random variables (such as \mathcal{S} and \mathcal{X}^s) are involved [25]. However, we know that $I(\mathbf{F}; \mathbf{S})$ ($I(\mathbf{F}; \mathbf{X}^s)$) is positive if and only if different realizations of \mathbf{F} can be estimated from realizations of \mathbf{S} (\mathbf{X}^s) more reliably than by randomly guessing. Adopting this operational perspective, let us consider a particular realization of \mathbf{F} , $\mathbf{f}(s)$, under which an observation s of \mathbf{S} was obtained and the following Bayesian inference problem²

$$\hat{\mathbf{f}}(s) = \max_{\mathbf{f}'} \Pr\{\mathbf{F} = \mathbf{f}' | \mathbf{S} = s\}, \quad (2)$$

where \mathbf{f}' represents any realization of \mathbf{F} . $\hat{\mathbf{f}}(s)$ is the Bayesian optimal (maximum *a posteriori*) estimator of $\mathbf{f}(s)$ and it specializes to the following maximum *a priori* estimator

$$\bar{\mathbf{f}} = \max_{\mathbf{f}'} \Pr\{\mathbf{F} = \mathbf{f}'\}, \quad (3)$$

if and only if \mathbf{F} and \mathbf{S} are statistically independent. Hence, if the estimation performance of $\hat{\mathbf{f}}$ is better than that of $\bar{\mathbf{f}}$, \mathbf{F} is a modulator of \mathcal{S} . The following corollary formalizes the necessary condition for \mathbf{F} to be a modulator according to Def. 1 that we have just found.

Corollary 1: Let (\mathbf{f}_n, s_n) , $n \in \mathbb{N}$, denote a sequence of samples independently drawn from the joint distribution of (\mathbf{F}, \mathbf{S}) and let $\mathbb{1}_A(\cdot)$ denote the indicator function for set A . If

$$\frac{1 - \Pr\{\hat{\mathbf{f}}(s_n) \neq \mathbf{f}_n\}}{1 - \Pr\{\bar{\mathbf{f}} \neq \mathbf{f}_n\}} = \lim_{N \rightarrow \infty} \frac{\frac{1}{N} \sum_{n=1}^N \mathbb{1}_{\{\mathbf{f}_n\}}(\hat{\mathbf{f}}(s_n))}{\frac{1}{N} \sum_{n=1}^N \mathbb{1}_{\{\mathbf{f}_n\}}(\bar{\mathbf{f}})} \quad (4)$$

$$\equiv \lim_{N \rightarrow \infty} \frac{A_N(\hat{\mathbf{f}})}{A_N(\bar{\mathbf{f}})} > 1,$$

\mathbf{F} is a modulator of \mathcal{S} .

$A_N(\hat{\mathbf{f}})$ as defined in the corollary denotes the *accuracy* of $\hat{\mathbf{f}}$ evaluated over N samples.

Since for practical applications only finitely many samples N and potentially suboptimal estimators, but not $\hat{\mathbf{f}}$, are available, we close this section by extending the strict notion of GBA modulation from Def. 1 with a relaxation of (4).

Definition 4 (Empirical GBA modulator): Let $\tilde{\mathbf{f}}$ denote any estimator of \mathbf{F} . If $\frac{A_N(\tilde{\mathbf{f}})}{A_N(\bar{\mathbf{f}})} > 1$ for N samples randomly drawn from the joint distribution of (\mathbf{F}, \mathbf{S}) , \mathbf{F} is an *empirical modulator (of degree N)* of \mathcal{S} .

IV. ANALYSIS

To overcome the problem that the optimal estimator $\hat{\mathbf{f}}$ is unknown in general, we use machine learning to train a suboptimal classifier on solving (2) approximately. Specifically, for discrete RVs F_j as assumed above, (2) constitutes a

²For the sake of brevity and readability, we focus on the modulation of \mathcal{S} for the rest of this section omitting \mathcal{X}^s and \mathcal{X}^c . However, the following discussion, including Corollary 1 and Def. 4, applies analogously to \mathcal{X}^s and \mathcal{X}^c instead of \mathcal{S} , if \mathbf{S} is replaced by \mathbf{X}^s and \mathbf{X}^c , respectively.

classification problem and we use an RF model trained on a finite set of data samples to solve it. RFs harness the collective intelligence of multiple decision trees for classification and prediction. Unlike other machine learning tools, RFs require minimal parameter tuning and are less prone to overfitting [26]. This makes RFs well suited for the small data sets used in this work.

We note that due to its potential suboptimality, the estimation performance achieved with the RF-based classifier constitutes a lower bound for the performance of $\hat{\mathbf{f}}$, if the considered data samples are representative of the true joint distribution of (\mathbf{F}, \mathbf{S}) . To ensure that the latter condition is fulfilled, we restrict the analysis to low-dimensional subsets $\mathbf{F} \subset \mathcal{F}$ and $\mathbf{S} \subset \mathcal{S}$ avoiding the curse of dimensionality [27]. To make this notion precise, we denote the RF-based estimator trained on any subset of bacterial species \mathbf{S} as $\hat{\mathbf{f}}_{\mathbf{S}}^{\text{RF}}(\mathbf{s})$ and define the optimal subset of features for RF-based classification as follows

$$\mathbf{S}^* = \arg \max_{\mathbf{S}' \subset \mathcal{S}} \mathbb{E}_{\mathcal{D}} A_N \left(\hat{\mathbf{f}}_{\mathbf{S}'}^{\text{RF}} \right), \quad (5)$$

where the expectation is over different partitionings $(\mathcal{T}_i, \mathcal{V}_i)$, $\mathcal{T}_i \cup \mathcal{V}_i = \mathcal{D}$, $\mathcal{T}_i \cap \mathcal{V}_i = \emptyset$, of the available data \mathcal{D} into training sets \mathcal{T}_i and test sets \mathcal{V}_i with $|\mathcal{V}_i| = N$. Exactly analogously to \mathbf{S}^* , $\mathbf{X}^{\text{s}*}$ and $\mathbf{X}^{\text{c}*}$ are defined as the optimal subsets of features from \mathcal{X}^{s} and \mathcal{X}^{c} , respectively.

In the following section, we will rigorously define $\hat{\mathbf{f}}^{\text{RF}}(\mathbf{s})$ and detail the strategy to determine \mathbf{S}^* ($\mathbf{X}^{\text{s}*}$, $\mathbf{X}^{\text{c}*}$) as well as the metrics used in this paper in order to assess its performance.

A. Random Forest Initialization and Training

When applying the RF classifier to a data set \mathcal{D} , $M = 100$ independent RF models are generated. To this end, \mathcal{D} is split into training and test sets $(\mathcal{T}_i, \mathcal{V}_i)$ according to a 3:1 ratio, where the splitting is done randomly for each RF. Since the splitting is independent of \mathbf{F} , it can potentially lead to unbalanced classes in \mathcal{T}_i and/or \mathcal{V}_i due to the typically small size of \mathcal{D} . Every factor $F_j \in \mathbf{F}$ corresponds to an individual class in the RF model.

Each RF model consists of $T = 100$ decision trees. Each tree in the forest is constructed using a random subset of \mathcal{T}_i . This method introduces diversity among the trees, which is critical for the model to generalize. Further randomness is introduced by selecting random subsets of maximum size $k = \sqrt{|\mathbf{S}|}$ from \mathbf{S} (or, analogously, of maximum size $k = \sqrt{|\mathbf{X}^{\text{s}}|}$ and $k = \sqrt{|\mathbf{X}^{\text{c}}|}$ from \mathbf{X}^{s} and \mathbf{X}^{c} , respectively) for each node split during tree construction. This feature selection is performed according to a splitting criterion called Gini impurity [28]. The Gini impurity is a popular choice due to its efficiency in measuring the disorder at a node, which helps in deciding which features are most favorable w.r.t. the final prediction accuracy. During RF training, the splitting at each decision tree is optimized. The RF implementation used to generate the results in this paper is based on the Python scikit-learn package [29].

B. Performance Metrics

In addition to the accuracy A_N as defined in Section III, we use the F1 score as additional performance metric. The F1 score balances recall $R = \frac{\text{TP}}{\text{TP} + \text{FN}}$ and precision $P = \frac{\text{TP}}{\text{TP} + \text{FP}}$ and is commonly used for assessing binary classification performance when datasets are unbalanced. Here, TP and FP denote true and false positives, respectively, and TN and FN denote true and false negatives, respectively. More specifically, F1 corresponds to the harmonic mean of precision and recall. Formally, the F1 score of any classifier $\hat{\mathbf{f}}$ for test set \mathcal{V}_i is defined as [30]

$$F1(\hat{\mathbf{f}}, \mathcal{V}_i) = 2 \frac{P \cdot R}{P + R} = \frac{2\text{TP}}{2\text{TP} + \text{FP} + \text{FN}}, \quad (6)$$

where P, R, TP, FP, TN, and FN are evaluated over all samples in \mathcal{V}_i . We note that $F1(\hat{\mathbf{f}}, \mathcal{V}_i)/F1(\mathbf{f}, \mathcal{V}_i) > 1$ implies $A_{|\mathcal{V}_i|}(\hat{\mathbf{f}})/A_{|\mathcal{V}_i|}(\mathbf{f}) > 1$, so the F1 score can be used instead of A_N to verify the condition in Def. 4 (for finite N).

C. Method for Selecting Important Features

After RF models have been trained on the full sets \mathcal{S} , \mathcal{X}^{s} , \mathcal{X}^{c} , we apply the permutation importance method [26, Chap. 10] to solve (5), i.e., to find \mathbf{S}^* , $\mathbf{X}^{\text{s}*}$, and $\mathbf{X}^{\text{c}*}$. To ensure that the importance ratings are reliable, we perform 10 random permutation tests for *each feature* for *each RF* model on the entire data set \mathcal{D} . The most important features \mathbf{S}^* , $\mathbf{X}^{\text{s}*}$, and $\mathbf{X}^{\text{c}*}$ are then selected as those features whose random permutation leads to the lowest mean accuracy.

V. DATA SOURCES

The proposed machine learning model is tested on four different peer-reviewed mouse datasets that are available online [23], [31]–[33]. All datasets study the impact of KD on either \mathcal{S} , \mathcal{X}^{s} , or \mathcal{X}^{c} . Table I lists the used datasets. Since the health status of the host is a potential GBA modulator, datasets from healthy (DS-2 [31] and DS-3 [32]) as well as from disease mouse models (DS-1 [23] and DS-4 [33]) are included. Specifically, the mice in [23] serve as animal models for DRE and a mouse model of human melanoma (skin cancer) is considered in [33]. Note that the sample sizes as reported in Table I are relatively small, ranging from $|\mathcal{D}| = 24$ to $|\mathcal{D}| = 125$, since they are obtained from animal models.

VI. EVALUATION

A. Impact of KD on the Gut Microbiota in a Mouse Model of Epilepsy

First, we study whether KD modulates \mathcal{S} in the mouse model of epilepsy. To this end, we consider the dataset from [23] (DS-1 in Table I) and train the RF model on predicting $\mathbf{F} = \{F_1\}$, where $F_1 \in \{\text{KD}, \text{ND}\}$, and $F_1 = \text{KD}$ for data samples from mice fed with KD and $F_1 = \text{ND}$ for mice fed with normal diet (ND). Applying the feature selection strategy detailed in IV-C, we obtain $\mathbf{S}^* = \{\text{Lactobacillaceae}, \text{Desulfovibrionaceae}, \text{Porphyromonadaceae}\}$, which is in agreement with previous studies [34], [35]. Fig. 2 illustrates how the features in \mathbf{S}^* are used to successfully classify the data samples into KD and ND. Specifically, it is evident from Fig. 2 that the mice from DS-1 can be perfectly clustered into KD and ND mice according to

Table I
DATA SETS

Type	Status	Sample Origin	$ \mathcal{S} $	$ \mathcal{X}^c $	$ \mathcal{X}^s $	\mathcal{F}	Sample size $ \mathcal{D} $	Index	Reference
Bacteria	Epilepsy	Fecal/Colon ^(a)	33 ^(b)	-	-	$\{\text{ND}, \text{KD}\} \times^{(c)} \{\text{D0}, \text{D4}, \text{D8}, \text{D14}\}^{(d)}$	3/3/3/3/3/3/3	DS-1	[23, Suppl. Table 2]
Metabolites	Healthy	Fecal	-	26	-	$\{\text{KD}, \text{ND}, \text{LCD}\}^{(e)}$	10/10/10	DS-2	[31, Suppl. Table 1]
Metabolites	Healthy	Intestinal	-	903	-	$\{\text{ND}, \text{HFD}, \text{KD}, \text{HK}\}^{(f)}$	6/6/6/6	DS-3	[32, Suppl. Table 4]
Metabolites	Cancer	Blood Plasma	-	-	75	$\{\text{A375}, \text{WM47}, \text{WM3311}, \text{WM3000}\}^{(g)}$ $\times \{\text{ND}, \text{KD1} + \text{KD2}\}^{(h)}$	13/11+10/10/7+7/ 10/11+10/12/12+12	DS-4	[33, Suppl. Table 2]

(a): There is no distinction between colon and fecal samples in the data set.
(b): Taxonomy level: Bacterial family level.
(c): \times denotes the Cartesian product.
(d): Day 0 (D0), Day 4 (D4), Day 8 (D8), Day 14 (D14).
(e): Low-carbohydrate diet (LCD), normal diet (ND).
(f): High-fat diet (HFD), high-fat to ketogenic conversion (HK).
(g): Human melanoma cell lines A375, WM47, WM3311, and WM3000.
(h): Long-chain triglyceride-based ketogenic diet (KD1) and Long-chain triglyceride-based ketogenic diet supplemented with C8 and C10 medium chain triglycerides (KD2) aggregated as $\text{KD} = \text{KD1} + \text{KD2}$.

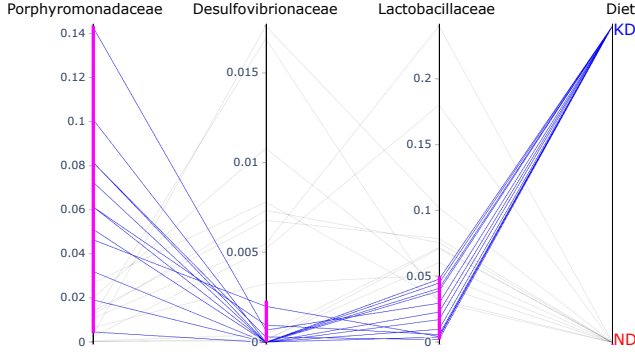


Figure 2. Relative abundances of the three most important bacterial species \mathbf{S}^* for discriminating KD and ND in the dataset from [23]. The three left-most vertical coordinate axes correspond to the three bacterial species in \mathbf{S}^* , the value of F_1 , KD or ND, is displayed on the right. Data samples are illustrated as blue and gray lines that interconnect the different coordinate axes. Blue lines correspond to data samples selected according to the intervals highlighted in pink.

the relative abundances of the gut bacteria in \mathbf{S}^* . The F1 score of the resulting RF model is 0.939053, exceeding by far the F1 score of 0.6 that is achieved with a model that classifies according to the majority class (either KD or ND in this case), i.e., \bar{f} , cf. (3). We conclude from Def. 4 that KD is an empirical GBA modulator. Since the diet is an externally controllable variable, KD is also a feasible, empirical GBA modulator for the epileptic mice from the dataset from [23].

B. Metabolomic Fingerprint of KD Compared to Other High-Fat, Low-Carbohydrate Diets in Healthy Mice

Next, we ask whether KD is distinguishable from other dietary interventions in terms of \mathcal{X}^c . To this end, we consider the datasets from [31] and [32] (DS-2 and DS-3, respectively, in Table I). Specifically, KD, low-carbohydrate diet (LCD), and ND are considered as dietary interventions in [31], while KD, high-fat diet (HFD), high-fat to ketogenic conversion (HK), and ND are considered in [32]. The metabolic profiles from [31] were obtained with a *targeted* assay, i.e., only the concentrations of $|\mathcal{X}^c| = 26$ preselected metabolites were measured. In contrast, the data from [32] was obtained in an *untargeted* manner, i.e., without preselecting specific metabolites, and comprises data for $|\mathcal{X}^c| = 903$ different metabolites.

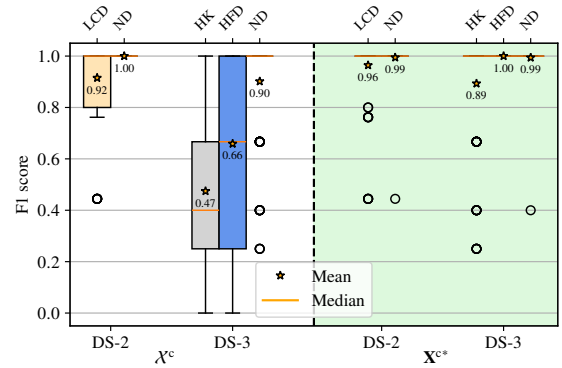


Figure 3. F1 scores for the different binary classification tasks KD vs. $\{\text{ND}, \text{LCD}, \text{HFD}, \text{HK}\}$. The boxplots depict the distributions of F1 scores across different partitionings of the datasets into training and test sets (the ratio of training samples to test samples remains fixed) for the complete set of colon metabolites \mathcal{X}^c (left, white background) and for the optimal subset of metabolites \mathbf{X}^{c*} (right, green background).

Fig. 3 illustrates the F1 scores obtained for these datasets for $M = 100$ different partitionings $(\mathcal{T}_i, \mathcal{V}_i)$ on the full set of colon metabolites \mathcal{X}^c as well as on the set of most important metabolites \mathbf{X}^{c*} . We observe from Fig. 3 that for DS-2 the RF classifier can distinguish very well between KD and ND as well as between KD and LCD based on both \mathcal{X}^c and \mathbf{X}^{c*} . Here, distinguishing LCD and KD is the more challenging task, since the LCD is more similar to the KD in nutrient composition as compared to ND. However, the performance of the RF model for DS-3 on \mathcal{X}^c is acceptable only for the simplest task, KD vs. ND. HK and HFD cannot be distinguished reliably based on \mathcal{X}^c . This outcome is expected, since HK and HFD are much similar to KD w.r.t. their respective nutrient composition as compared to ND. Finally, we observe from Fig. 3 that all different diets can perfectly be distinguished from KD based on the important factors \mathbf{X}^{c*} with median F1 scores identical to 1. This result has two important consequences. First, the KD modulates \mathcal{X}^c according to Defs. 1 and 4. Second, the important factor selection strategy adopted in this paper can effectively compensate the curse of dimensionality that otherwise arises in the high-dimensional data space of DS-3.

Table II
F1 SCORES FOR DIFFERENT TRAIN (COLUMNS) AND TEST (ROWS)
CONDITIONS (DS-4)

serum	A375	WM3000	WM3311	WM47
A375	1.00	0.89	0.97	1.00
WM3000	0.99	1.00	0.93	0.99
WM3311	0.75	0.88	1.00	0.93
WM47	1.00	0.96	0.76	1.00

C. Metabolomic Fingerprint of KD in a Mouse Model of Cancer

Finally, we study the impact of the KD on \mathcal{X}^s in a mouse model of human melanoma [33] (DS-4 in Table I). Specifically, we ask two questions, namely (i) whether KD and/or cancer type (A375, WM47, WM3311, WM3000) are (empirical) modulators of \mathcal{X}^s and (ii) whether the impact of KD on \mathcal{X}^s is the same irrespective of the type of cancer the host has.

To answer the first question, we evaluated the F1 scores of RF models trained to classify the type of diet and the type of cancer, respectively. For diet prediction, the model achieved a median F1 score of 0.97, and an accuracy of > 0.98 for cancer type prediction (after reducing the feature space to \mathbf{X}^{s*}). Hence, both KD and cancer type modulate \mathcal{X}^s (empirically) according to Def. 4, though from the two only KD is a feasible modulator, cf. Def. 2.

To answer the second question, we trained different RF models to classify KD vs. ND for specific types of cancer. In this way, we obtain 4 different estimators $\hat{\mathbf{f}}_{\text{A375}}^{\text{RF}}$, $\hat{\mathbf{f}}_{\text{WM47}}^{\text{RF}}$, $\hat{\mathbf{f}}_{\text{WM3311}}^{\text{RF}}$, and $\hat{\mathbf{f}}_{\text{WM3000}}^{\text{RF}}$, where each of these was trained on data samples with the cancer type indicated in the subscript and the respective optimal sets of serum metabolites \mathbf{X}^{s*} denoted in the following as $\mathbf{X}_{\text{A375}}^{s*}$, $\mathbf{X}_{\text{WM47}}^{s*}$, $\mathbf{X}_{\text{WM3000}}^{s*}$, and $\mathbf{X}_{\text{WM3311}}^{s*}$. The performance of each of these estimators is then evaluated on test data samples with the same cancer type and on data samples with different cancer types. Table II summarizes the resulting mean F1 scores.

First, we observe from Table II that each estimator works perfectly (F1 score identical to 1) on data with the same cancer type as it was trained on. Hence, we conclude that KD is a robust GBA modulator according to Def. 3, where, here, $\mathbf{F}_1 = \{\text{KD}, \text{ND}\}$ and $\mathbf{F}_2 = \{\text{A375}, \text{WM47}, \text{WM3311}, \text{WM3000}\}$. Second, we observe from Table II that the estimation performance of each estimator deteriorates when applied to data samples with other cancer types. For example, $\hat{\mathbf{f}}_{\text{A375}}^{\text{RF}}$ achieves only a mean F1 score of 0.75 when applied to data of cancer type WM3000. This observation points towards differences in how KD modulates the GBA depending on the cancer type.

To further elucidate this relationship, we study $\mathbf{X}_{\text{A375}}^{s*}$, $\mathbf{X}_{\text{WM47}}^{s*}$, $\mathbf{X}_{\text{WM3000}}^{s*}$, $\mathbf{X}_{\text{WM3311}}^{s*}$ in the following. Fig. 4 illustrates how the important factors identified via (5) cluster the data points for each cancer type. Specifically, we observe from Fig. 4 that \mathbf{X}^{s*} provides a clearly visible clustering of the data samples for each cancer type (top panels in Fig. 4), whereas no such cluster structures are recognizable for a random selection of factors (bottom panels in Fig. 4). Furthermore, we identified

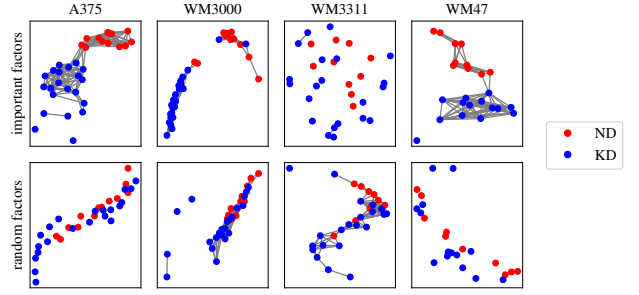


Figure 4. Network plot based on the similarity of the data samples from DS-4 w.r.t. the important factors \mathbf{X}^{s*} (top) and a random selection of $|\mathbf{X}^{s*}|$ (bottom) factors from \mathcal{X}^s . Blue and red dots indicate data samples with KD and ND, respectively.

the following important factors

$$\mathbf{X}_{\text{A375}}^{s*} = \{\alpha\text{-Aminoadipic acid, 1-Methylhistidine, } \beta\text{-Aminobutyric acid, Proline Betaine}\}, \quad (7)$$

$$\mathbf{X}_{\text{WM47}}^{s*} = \{\alpha\text{-Aminoadipic acid, } \beta\text{-Aminobutyric acid, EPA, 1-Methylhistidine}\}, \quad (8)$$

$$\mathbf{X}_{\text{WM3000}}^{s*} = \{\beta\text{-Aminobutyric acid, 1-Methylhistidine, DHA, Threonine}\}, \quad (9)$$

$$\mathbf{X}_{\text{WM3311}}^{s*} = \{\text{Lysine, } \alpha\text{-Aminoadipic acid, Tryptophan, Glutamine}\}. \quad (10)$$

We conclude that some serum metabolites, such as α -Aminoadipic acid, 1-Methylhistidine, and β -Aminobutyric acid, appear to be indicative of KD irrespective of the cancer type and these findings are in line with what has been previously shown by others [36] and in general with the effect of KD on aminoacids metabolisms [37]. However, other metabolites are informative of KD only for specific cancer types, such as Proline Betaine for A375, EPA for WM47, DHA and Threonine for WM3000, and Lysine, Tryptophan, and Glutamine for WM3311. This finding is in line with previous evidence of KD effect on Tryptophan metabolism [7] and aminoacids metabolisms [37].

VII. CONCLUSION

In this paper, we present a novel framework for GBA-MC. The framework defines formal criteria for identifying potential therapeutic targets for GBA-based treatment of neurological diseases. To demonstrate the applicability of the general model to real-world data, we developed a machine learning approach and examined the effects of dietary interventions, particularly the KD, on the gut microbiome and metabolic profiles of healthy and diseased mice. Using the proposed approach, we confirmed the role of the KD as a potential therapeutic target that modulates GBA. The proposed model could also identify specific bacterial species and metabolites likely to play a major role in mediating the impact of the KD on the host. These findings open up promising avenues for further research on the design of highly effective, personalized dietary interventions for treating neurological disorders.

REFERENCES

- [1] I. F. Akyildiz, M. Pierobon, S. Balasubramaniam, and Y. Koucheryavy, "The Internet of Bio-Nano Things," *IEEE Commun. Mag.*, vol. 53, no. 3, pp. 32–40, Mar. 2015.

- [2] U. A. Chude-Okonkwo, R. Malekian, B. T. Maharaj, and A. V. Vasilakos, "Molecular communication and nanonetwork for targeted drug delivery: A survey," *IEEE Commun. Surv. Tut.*, vol. 19, no. 4, pp. 3046–3096, May 2017.
- [3] Y. Chahibi, M. Pierobon, S. O. Song, and I. F. Akyildiz, "A molecular communication system model for particulate drug delivery systems," *IEEE Trans. Biomed. Eng.*, vol. 60, no. 12, pp. 3468–3483, Jun. 2013.
- [4] T. G. Dinan and J. F. Cryan, "The microbiome-gut-brain axis in health and disease," *Gastroenterol. Clin. N. Am.*, vol. 46, no. 1, pp. 77–89, Mar. 2017.
- [5] I. F. Akyildiz *et al.*, "Microbiome-gut-brain axis as a biomolecular communication network for the Internet of Bio-Nano Things," *IEEE Access*, vol. 7, pp. 136 161–136 175, Sep. 2019.
- [6] S. S. Somathilaka, D. P. Martins, W. Barton, O. O'Sullivan, P. D. Cotter, and S. Balasubramaniam, "A graph-based molecular communications model analysis of the human gut bacteriome," *IEEE J. Biomed. Health Informatics*, vol. 26, no. 7, pp. 3567–3577, 2022.
- [7] D. Effinger *et al.*, "A ketogenic diet substantially reshapes the human metabolome," *Clin. Nutr.*, vol. 42, no. 7, pp. 1202–1212, Jul. 2023.
- [8] L. F. Iannone *et al.*, "Microbiota-gut brain axis involvement in neuropsychiatric disorders," *Expert Rev. Neurother.*, vol. 19, no. 10, pp. 1037–1050, Oct. 2019.
- [9] G. R. Lum *et al.*, "Ketogenic diet therapy for pediatric epilepsy is associated with alterations in the human gut microbiome that confer seizure resistance in mice," *Cell Rep.*, vol. 42, no. 12, p. 113521, Dec. 2023.
- [10] A. J. Macpherson and N. L. Harris, "Interactions between commensal intestinal bacteria and the immune system," *Nat. Rev. Immunol.*, vol. 4, no. 6, pp. 478–485, Jun. 2004.
- [11] G. Singh and J. W. Sander, "The global burden of epilepsy report: Implications for low- and middle-income countries," *Epilepsy Behav.*, vol. 105, p. 106949, Apr. 2020.
- [12] J. I. Sirven, "Epilepsy: A spectrum disorder," *Cold Spring Harb. Perspec. Med.*, vol. 5, no. 9, p. a022848, Sep. 2015.
- [13] L. A. David *et al.*, "Diet rapidly and reproducibly alters the human gut microbiome," *Nature*, vol. 505, no. 7484, pp. 559–563, Jan. 2014.
- [14] F. De Vadder *et al.*, "Microbiota-generated metabolites promote metabolic benefits via gut-brain neural circuits," *Cell*, vol. 156, no. 1, pp. 84–96, Jan. 2014.
- [15] A. Zhernakova *et al.*, "Population-based metagenomics analysis reveals markers for gut microbiome composition and diversity," *Science*, vol. 352, no. 6285, pp. 565–569, Apr. 2016.
- [16] P. J. Turnbaugh, V. K. Ridaura, J. J. Faith, F. E. Rey, R. Knight, and J. I. Gordon, "The effect of diet on the human gut microbiome: A metagenomic analysis in humanized gnotobiotic mice," *Sci. Transl. Med.*, vol. 1, no. 6, pp. 6ra14–6ra14, Nov. 2009.
- [17] G. Falony *et al.*, "Population-level analysis of gut microbiome variation," *Science*, vol. 352, no. 6285, pp. 560–564, Apr. 2016.
- [18] L. Diaz-Marugan, J. B. Kantsjö, A. Rutsch, and F. Ronchi, "Microbiota, diet, and the gut-brain axis in multiple sclerosis and stroke," *Eur. J. Immunol.*, vol. 53, no. 11, p. 2250229, Nov. 2023.
- [19] M. Ceccon, J. B. Kantsjö, and F. Ronchi, "Personalized paths: Unlocking alzheimer's via the gut-brain axis," *Vis. Med.*, vol. 40, no. 4, pp. 194–209, Aug. 2024.
- [20] A. Peng *et al.*, "Altered composition of the gut microbiome in patients with drug-resistant epilepsy," *Epilepsy Res.*, vol. 147, no. 102, pp. 102–107, Nov. 2018.
- [21] X. Gong *et al.*, "Alteration of gut microbiota in patients with epilepsy and the potential index as a biomarker," *Front. Microbiol.*, vol. 11, p. 517797, Sep. 2020.
- [22] Y. Zhang, S. Zhou, Y. Zhou, L. Yu, L. Zhang, and Y. Wang, "Altered gut microbiome composition in children with refractory epilepsy after ketogenic diet," *Epilepsy Res.*, vol. 145, pp. 163–168, Sep. 2018.
- [23] C. A. Olson, H. E. Vuong, J. M. Yano, Q. Y. Liang, D. J. Nusbaum, and E. Y. Hsiao, "The gut microbiota mediates the anti-seizure effects of the ketogenic diet," *Cell*, vol. 173, no. 7, pp. 1728–1741, Jun. 2018.
- [24] M. Dahlin, C. E. Wheelock, and S. Prast-Nielsen, "Association between seizure reduction during ketogenic diet treatment of epilepsy and changes in circulatory metabolites and gut microbiota composition," *eBioMedicine*, vol. 109, p. 105400, Nov. 2024.
- [25] M. S. Roulston, "Estimating the errors on measured entropy and mutual information," *Phys. D: Nonlinear Phenom.*, vol. 125, no. 3–4, pp. 285–294, Sep. 1999.
- [26] L. Breiman, "Random forests," *Mach. Learn.*, vol. 45, pp. 5–32, Oct. 2001.
- [27] R. Bellman, *Dynamic Programming*, ser. Princeton Landmarks in Mathematics and Physics. Princeton, NJ, USA: Princeton University Press, 2021.
- [28] P. Probst, M. N. Wright, and A.-L. Boulesteix, "Hyperparameters and tuning strategies for random forest," *Wiley Interdiscip. Rev.: Data Min. Knowl. Discov.*, vol. 9, no. 3, p. e1301, Jan. 2019.
- [29] "Random forest classifier," 2025. [Online]. Available: <https://scikit-learn.org/stable/modules/generated/sklearn.ensemble.RandomForestClassifier.html>
- [30] B. J. Erickson and F. Kitamura, "Magician's corner: 9. performance metrics for machine learning models," *Radiol. Artif. Intell.*, vol. 3, no. 3, p. e200126, May 2021.
- [31] C. Kong *et al.*, "Ketogenic diet alleviates colitis by reduction of colonic group 3 innate lymphoid cells through altering gut microbiome," *Signal Transduct. Target. Ther.*, vol. 6, no. 1, p. 154, Apr. 2021.
- [32] H. Qiu *et al.*, "Metagenomic and metabolomic analysis showing the adverse risk–benefit trade-off of the ketogenic diet," *Lipids Health Dis.*, vol. 23, no. 1, p. 207, Jun. 2024.
- [33] D. D. Weber *et al.*, "Ketogenic diets slow melanoma growth in vivo regardless of tumor genetics and metabolic plasticity," *Cancer Metab.*, vol. 10, no. 1, p. 12, Jul. 2022.
- [34] M. Alexander *et al.*, "A diet-dependent host metabolite shapes the gut microbiota to protect from autoimmunity," *Cell Rep.*, vol. 43, no. 11, Nov. 2024.
- [35] A. Paoli, L. Mancin, A. Bianco, E. Thomas, J. F. Mota, and F. Piccini, "Ketogenic diet and microbiota: Friends or enemies?" *Genes*, vol. 10, no. 7, p. 534, Jul. 2019.
- [36] H. Peng, M. Fu, and J. Li, "New perspectives: The impact of ketogenic diet on the immune system," *Signal Transduct. Target. Ther.*, vol. 10, no. 1, pp. 1–2, Apr. 2025.
- [37] M. Yudkoff, Y. Daikhin, T. M. Melø, I. Nissim, U. Sonnewald, and I. Nissim, "The ketogenic diet and brain metabolism of amino acids: Relationship to the anticonvulsant effect," *Annu. Rev. Nutr.*, vol. 27, no. 1, pp. 415–430, Aug. 2007.